

Eemian and Holocene climate

N. Fischer and
J. H. Jungclaus

This discussion paper is/has been under review for the journal *Climate of the Past* (CP).
Please refer to the corresponding final paper in CP if available.

Evolution of the seasonal temperature cycle in a transient Holocene simulation: orbital forcing and sea-ice

N. Fischer^{1,2} and J. H. Jungclaus¹

¹Max Planck Institute for Meteorology, Bundesstrasse 53, 20146 Hamburg, Germany

²International Max Planck Research School for Earth System Modelling, Hamburg, Germany

Received: 19 January 2011 – Accepted: 20 January 2011 – Published: 3 February 2011

Correspondence to: N. Fischer (nils.fischer@zmaw.de)

Published by Copernicus Publications on behalf of the European Geosciences Union.

Title Page

Abstract

Introduction

Conclusions

References

Tables

Figures

⏪

⏩

◀

▶

Back

Close

Full Screen / Esc

Printer-friendly Version

Interactive Discussion



Abstract

Changes in the Earth's orbit lead to changes in the seasonal and meridional distribution of insolation. We quantify the influence of orbitally induced changes on the seasonal temperature cycle in a transient simulation of the last 6000 years – from the mid-Holocene to today – using a coupled atmosphere-ocean general circulation model (ECHAM5/MPI-OM) including a land surface model (JSBACH).

The seasonal temperature cycle responds directly to the insolation changes almost everywhere. In the Northern Hemisphere, its amplitude decreases according to an increase in winter insolation and a decrease in summer insolation. In the Southern Hemisphere, the opposite is true.

Over the Arctic Ocean, however, decreasing summer insolation leads to an increase of sea-ice cover. The insulating effect of sea ice between the ocean and the atmosphere favors more continental conditions over the Arctic Ocean in winter, resulting in strongly decreasing temperatures. Consequently, there are two competing effects: the direct response to insolation changes and a sea-ice dynamics feedback. The sea-ice feedback is stronger, and thus an increase in the amplitude of the seasonal cycle over the Arctic Ocean occurs. This increase is strongest over the Barents Shelf and influences the temperature response over northern Europe.

We compare our modelled seasonal temperatures over Europe to paleo reconstructions. We find better agreements in winter temperatures than in summer temperatures and better agreements in northern Europe than in southern Europe, since the model does not reproduce the southern European Holocene summer cooling inferred from the paleo data. The temperature reconstructions for northern Europe support the notion of the influence of the sea-ice effect on the evolution of the seasonal temperature cycle.

CPD

7, 463–483, 2011

Eemian and Holocene climate

N. Fischer and
J. H. Jungclauss

Title Page

Abstract

Introduction

Conclusions

References

Tables

Figures



Back

Close

Full Screen / Esc

Printer-friendly Version

Interactive Discussion



1 Introduction

The amplitude of the seasonal temperature cycle depends on changes in the Earth's orbital parameters that alter the seasonal and the meridional distribution of insolation. The orbital forcing constitutes the dominant natural long-term climate forcing in the last 6000 years, from the mid-Holocene to today (e.g., Wanner et al., 2008; Renssen et al., 2009). On millennial time-scales, the insolation changes are due to the precession of the Earth's elliptical orbit around the Sun and the changes in obliquity of the Earth's rotation axis with respect to the orbital plane.

The Earth's obliquity was larger 6000 years ago and, at the same time, summer solstice was closer to perihelion. In the Northern Hemisphere, this resulted in higher insolation in summer and lower insolation in winter, and consequently, in increased seasonality. Although these changes in insolation were small in the annual mean ($<4.5 \text{ W/m}^2$ at high latitudes), feedbacks between the different components of the Earth system amplify or dampen the insolation signal. This leads to changes in climate also on time-scales longer than seasonal as has been shown in several time-slice simulation studies (e.g. Braconnot et al., 2007a; Otto et al., 2009). The annual temperature change is caused by seasonal temperature changes that vary in their individual amplitudes. Therefore, the annual signal can be dominated by one particular season, and hence, by seasonality.

Denton et al. (2005) discuss the role of seasonality in abrupt climate change events during the last 60 000 years by means of temperature reconstructions from ice cores and glacier advances in Greenland. The authors found that during abrupt cold climate events the annual temperature anomalies in high northern latitudes are dominated by the winter temperature anomalies that are caused by increased winter sea-ice cover in the Northern Hemisphere. This leads to continental conditions over large parts of the northern high latitudes and thus to an increase in the amplitude of the seasonal temperature cycle.

Eemian and Holocene climate

N. Fischer and
J. H. Jungclauss

Title Page

Abstract

Introduction

Conclusions

References

Tables

Figures



Back

Close

Full Screen / Esc

Printer-friendly Version

Interactive Discussion



Eemian and Holocene climate

N. Fischer and
J. H. Jungclauss

Title Page

Abstract

Introduction

Conclusions

References

Tables

Figures



Back

Close

Full Screen / Esc

Printer-friendly Version

Interactive Discussion



In this study, we investigate how changes in seasonality affect the mean climate evolution from the mid-Holocene to today. Given the seasonal distribution of insolation in the Northern Hemisphere in the mid-Holocene, the expected direct response is a decrease in the amplitude of the seasonal cycle in the course of the last 6000 years.

Nevertheless, sea-ice evolution over the Arctic Ocean and the interaction between atmosphere, ocean and sea ice, may alter this direct response. We present the evolution of the seasonal temperature cycle over the last 6000 years in a coupled atmosphere-ocean model with an integrated dynamic land surface model and compare the results to Holocene temperature reconstructions obtained from pollen archives.

2 Model setup and experimental design

We perform a 6000-year-long transient simulation with the coupled atmosphere-ocean general circulation model ECHAM5/MPI-OM (Jungclauss et al., 2006) including the land surface model JSBACH (Raddatz et al., 2007) with a dynamic vegetation module (Brovkin et al., 2009). The atmosphere component ECHAM5 (Roeckner et al., 2003) is run in resolution T31 (corresponding to 3.75°) and the ocean component MPI-OM (Marsland et al., 2003) is run in resolution GR30 (corresponding to $\sim 3^\circ$). The ocean model component includes a Hibler-type zero-layer dynamic-thermodynamic sea-ice model with viscous-plastic rheology (Semtner, 1976; Hibler, 1979).

Since we are mainly interested in the effects of orbital forcing on the evolution of the seasonal temperature cycle, we do not apply further external forcing such as solar, volcanic, or greenhouse gases and set greenhouse gases to pre-industrial values (CO_2 to 280 ppm, CH_4 to 700 ppb, N_2O to 265 ppb). Thus we do not expect the model results to perfectly match climate reconstructions. Rather, we are interested in finding mechanisms that determine the changes in the seasonal temperature cycle from the mid-Holocene to today. We apply orbital forcing on a yearly basis following VSOP87 (Bretagnon and Francou, 1988) implemented in the radiation scheme of the atmosphere model component. We do not apply any acceleration technique and can thus

analyze the ocean's response to changes in insolation on orbital timescales. We initialize the transient experiment from a 3500-year-long mid-Holocene (6000 years before present) time-slice simulation with orbital forcing presented in an earlier study (Fischer and Jungclaus, 2010). For the following analysis we use monthly mean output from both the atmosphere and the ocean model.

3 Results and discussion

3.1 Seasonal insolation and sea ice effects

We define the amplitude of the seasonal temperature cycle (STCA) as the surface temperature difference between the coldest and the warmest month of the year. Similarly, we define the amplitude of the seasonal insolation cycle (SICA) as the difference between annual maximum and minimum incoming short wave radiation on a monthly mean basis. SICA depends on the external orbital forcing only. Figure 1a and c show zonally averaged Hovmoeller-type diagrams of SICA and STCA, respectively. Changes in STCA follow those in SICA qualitatively with the exception of the high northern latitudes where, despite decreasing SICA, STCA increases. The maximal STCA response in the low- and mid latitudes in the Northern Hemisphere (NH) is shifted northwards from 15° to 40° N for the maximum decrease in STCA and southwards from 15° to 30° S for the low- and mid latitudes increase in STCA in the Southern Hemisphere (SH). The difference between SICA and STCA in low- and mid latitudes can be attributed to planetary albedo effects. Figure 1b shows the evolution of the net incoming short wave radiation seasonal cycle amplitude (net SICA) that includes the planetary albedo effect and that corresponds more closely to STCA. The difference between SICA and net SICA in low- and mid latitudes occurs because of a southward shift of the intertropical convergence zone (ITCZ) over Africa (calculated after Braconnot et al., 2007b) and thus a decrease in cloud cover over the NH low latitudes and an increase in the SH ITCZ region. Nevertheless, the increase in STCA at high northern latitudes cannot be

Eemian and Holocene climate

N. Fischer and
J. H. Jungclaus

Title Page

Abstract

Introduction

Conclusions

References

Tables

Figures



Back

Close

Full Screen / Esc

Printer-friendly Version

Interactive Discussion



explained by net SICA which decreases at high northern latitudes. This is also true for the SH high latitudes, where the increase in STCA is disproportional to the increase in SICA and net SICA.

A spatially resolved plot of linear trends in STCA (Fig. 2) shows that the increase in STCA at high northern latitudes is confined to the Arctic Ocean, with the strongest signal over the Barents Shelf. This zonal mean increase outweighs the decrease in STCA over the continents at the same latitude bands. The expansion of sea ice is the most likely cause for the signal. Decreasing summer insolation in the high northern latitudes reduces summer sea-ice melt. In the Arctic Ocean, sea-ice cover increases from 90 to 95% in the annual mean (Fig. 3), mainly because of an increase in summer sea-ice cover. Because of the heat insulating effect of sea ice, the ocean cannot act as a reservoir gaining heat in the summer months and releasing it in the winter months, and thus, it dampens STCA. The annual mean atmosphere-ocean heat flux over the Arctic (positive values indicate heat flux directed from the atmosphere to the ocean), decreases in absolute values by 13% from -7.4 to -6.6 W/m^2 . The seasonal cycle of heat flux over the Arctic Ocean (Fig. 3) decreases by 22% with the summer heat flux decreasing from 70 to 52 W/m^2 (24%) and the winter heat flux decreasing in absolute values from -36 to -28 W/m^2 (22%).

The decrease in the amplitude of the seasonal cycle of sea-ice is due to an increase in summer sea-ice cover and the continental boundaries of the Arctic Ocean basin that limit winter sea-ice extent when the whole basin is sea-ice covered.

In the high southern latitudes, over the Southern Ocean and Antarctica, as opposed to the Arctic region, the sea-ice effect amplifies the changes in insolation. The increase in STCA over the Southern Ocean is stronger than the increase over Antarctica (Fig. 2). Austral summer insolation at high southern latitudes increases by only 5 W/m^2 and insolation changes in austral autumn and winter are less than 2 W/m^2 (Fig. 4). A strong decrease of 16 W/m^2 occurs in austral spring, which leads to an increase in maximum sea-ice extent. The increased austral summer insolation leads to stronger ice melt and consequently, to an increase in the amplitude of the seasonal cycle of sea ice, despite

Eemian and Holocene climate

N. Fischer and
J. H. Jungclauss

Title Page

Abstract

Introduction

Conclusions

References

Tables

Figures



Back

Close

Full Screen / Esc

Printer-friendly Version

Interactive Discussion



the fact that the minimal sea-ice extent in the late Holocene is larger than in the mid-Holocene. The increase in the amplitude of the seasonal sea-ice cycle then amplifies the increase in STCA.

Over the NH continents and sub-Arctic oceans, STCA decreases according to the decrease in SICA, with the strongest decrease over North Africa, the northern part of the Arabian Peninsula and central Asia. In the SH, STCA increases over the oceans and Australia, but decreases over South America and southern Africa probably due to the southward shift of the ITCZ. Thus, we find two effects determining STCA in the mid- and late Holocene: seasonal insolation distribution and sea-ice cover.

To investigate what effect and also what season is dominating the changes in STCA we have a closer look at the annual mean temperature evolution. Zonal changes in surface temperature, an increase at low latitudes, and a decrease in high latitudes (Fig. 5), correspond to the changing insolation distribution with increasing insolation around the equator in boreal winter and decreasing insolation at high northern latitudes in boreal summer. In the low latitudes, the insolation induced warming in winter is accompanied by a southward migration of the ITCZ, which leads to a strong decrease in cloud cover and precipitation in the monsoon season from late summer to autumn both over the Indian sub-continent and the Sahel region. Due to these two effects the warming signal is present the whole year. The STCA decrease is strongest just north of these warming regions and is dominated by the insolation changes: an increase in summer insolation and thus temperature, and a decrease in both in winter.

In the Arctic Ocean, especially over the Barents Shelf and along the east coast of Greenland, cooling is enhanced where sea ice is expanding. The cooling signal is strongest in autumn and in winter, when – compared to the mid-Holocene conditions – sea-ice cover acts as an insulator and heat flux between the ocean and the atmosphere is inhibited. Thus, the autumn and winter temperatures sink, despite the fact that winter insolation is not changing significantly. So the sea-ice effect dominates the STCA. This is similar to the mechanism proposed to explain the abrupt climate changes in the last 60 000 years in Denton et al. (2005). Extensive winter sea-ice cover in the

Eemian and Holocene climate

N. Fischer and
J. H. Jungclauss

Title Page

Abstract

Introduction

Conclusions

References

Tables

Figures



Back

Close

Full Screen / Esc

Printer-friendly Version

Interactive Discussion



Arctic Ocean, leads to continental climate conditions over the Arctic region and cooler winters in the late Holocene compared to the mid-Holocene, when reduced sea-ice cover and thus open ocean in the Arctic region acts as a heat reservoir and thus leads to warmer winters. This affects not only the Arctic Ocean, but also influences the adjacent continents. This effect could be amplified by a synergy of the sea-ice effect and the snow-albedo feedback due to the shift of the northern tree-line in the Holocene. The strength of this synergetic effect in the model setup used here, however, has been shown to be small (Otto et al., 2009).

3.2 Comparison with temperature reconstructions for Europe

We compare the model results with the reconstruction of European winter and summer temperatures inferred from 620 pollen archives by Davis et al. (2003). In their paper, the authors sub-divide the European continent into six zones: northern, central, and southern Europe, with an eastern and western part each. Since the resolution of our model is quite coarse we discuss only changes for northern and southern Europe and the respective western and eastern parts, with 15° E being the boundary between east and west and 50° N being the boundary between northern and southern Europe.

The model results agree with the reconstructed data in trend and amplitude in north-eastern European summer and southeastern European winter. Qualitatively, the model reproduces the reconstructed temperatures in northeastern European summer and winter temperatures in southern Europe, but with different amplitudes. The most obvious discrepancy appears to be in southern European summer temperatures, where the model results exhibit a decrease and the reconstructed temperatures an increase, but also northern European winter temperatures differ between model and reconstructions.

In a recent study, Davis and Brewer (2009) find the same discrepancies when they compare their reconstructed data to Holocene time-slice model results from the PMIP2-exercise (Braconnot et al., 2007a). Davis and Brewer (2009) attribute the discrepancies to how climate models simulate the response of the latitudinal temperature gradient

CPD

7, 463–483, 2011

Eemian and Holocene climate

N. Fischer and
J. H. Jungclauss

Title Page

Abstract

Introduction

Conclusions

References

Tables

Figures



Back

Close

Full Screen / Esc

Printer-friendly Version

Interactive Discussion



(LTG) between mid and high northern latitudes to a changing latitudinal insolation gradient (LIG) (Raymo and Nisancioglu, 2003).

Davis and Brewer (2009) define the LIG and the LTG as the difference between the latitude bands 30–45° N and 55–75° N in insolation and temperature, respectively, and show that reconstructed Holocene temperatures follow this seasonal LIG very closely (Fig. 7a).

For the modelled seasonal temperature gradients of the present study, however, this is only true for the winter, whereas the summer LTG is strongly divergent from the summer LIG (Fig. 7b).

Summer LTG calculated from European temperature differences for late spring season (April to June), does resemble the LIG. But since other independent methods such as pollen-climate reconstruction based on inverse modelling approaches to reconstructing mid-Holocene climate (Wu et al., 2007) indicate a Holocene summer cooling as well, this temporal shift is a rather improbable solution to the problem.

The modelled summer LTG follows the LIG if all continents are considered (Fig. 7c), although the trend in the summer LTG in the model is weaker than the pollen-reconstructed trend in LTG. For the pollen-reconstructed temperatures, the argument of LTG sensitivity to LIG is shown to be valid for all Northern Hemisphere continents as well (Davis et al., 2011). It is possible that the discrepancy between reconstructed and modelled European temperatures is due to the coarse resolution of the model, that is not resolving changes in the atmospheric circulation induced by insolation changes correctly. The discrepancy could also result from a feedback or mechanism that is missing in the model. The missing summer cooling signal in southern Europe and the Mediterranean region is not specific for the model setup used in this study, but it is a common feature of coupled climate models (Braconnot et al., 2007b) in all of which mid-Holocene cooling is confined to the monsoon regions. This low latitude summer cooling is related to the strength of the reconstructed summer LTG trend and can explain the difference in amplitude compared to the modelled summer LTG strength.

Eemian and Holocene climate

N. Fischer and
J. H. Jungclauss

Title Page

Abstract

Introduction

Conclusions

References

Tables

Figures

⏪

⏩

◀

▶

Back

Close

Full Screen / Esc

Printer-friendly Version

Interactive Discussion



**Eemian and
Holocene climate**N. Fischer and
J. H. Jungclauss

Title Page

Abstract

Introduction

Conclusions

References

Tables

Figures

◀

▶

◀

▶

Back

Close

Full Screen / Esc

Printer-friendly Version

Interactive Discussion



and diminishes the seasonal temperature cycle amplitude's decrease on the adjacent continents. Annual mean temperature changes in the high northern latitudes are dominated by a decrease in winter temperatures, whereas summer temperatures decrease to a lesser extent. Comparison of the model results to a reconstruction from paleo archives also indicates an influence of sea-ice evolution on the seasonal temperature cycle amplitude. Discrepancies between the reconstruction and the model results are most obvious in the southern European summer, where the model does not reproduce the mid-Holocene cooling inferred from various climate proxies. On the global scale, the modelled response in the latitudinal temperature gradient to the latitudinal insolation gradient matches the reconstructed response, suggesting, that the coarse resolution version of the model might be responsible for the mismatch. Nevertheless, the low latitude summer cooling inferred from pollen reconstructions is not captured by the model.

The service charges for this open access publication have been covered by the Max Planck Society.

Acknowledgements. This work has been performed within the priority program INTERDY-NAMIK of the German Research Foundation (DFG). The model integration was performed on the Linux-cluster of the German Climate Computing Center (DKRZ) in Hamburg. We would like to thank Basil Davis for providing the data-set for the Holocene temperature reconstruction in Europe and very helpful comments on an earlier version of the manuscript.

References

Braconnot, P., Otto-Bliesner, B., Harrison, S., Joussaume, S., Peterchmitt, J.-Y., Abe-Ouchi, A., Crucifix, M., Driesschaert, E., Fichet, Th., Hewitt, C. D., Kageyama, M., Kitoh, A., L  n  , A., Loutre, M.-F., Marti, O., Merkel, U., Ramstein, G., Valdes, P., Weber, S. L., Yu, Y., and Zhao, Y.: Results of PMIP2 coupled simulations of the Mid-Holocene and Last Glacial Maximum – Part 1: experiments and large-scale features, *Clim. Past*, 3, 261–277, doi:10.5194/cp-3-261-2007, 2007a. 465, 470

- Braconnot, P., Otto-Bliesner, B., Harrison, S., Joussaume, S., Peterchmitt, J.-Y., Abe-Ouchi, A., Crucifix, M., Driesschaert, E., Fichetef, Th., Hewitt, C. D., Kageyama, M., Kitoh, A., Loutre, M.-F., Marti, O., Merkel, U., Ramstein, G., Valdes, P., Weber, L., Yu, Y., and Zhao, Y.: Results of PMIP2 coupled simulations of the Mid-Holocene and Last Glacial Maximum – Part 2: feedbacks with emphasis on the location of the ITCZ and mid- and high latitudes heat budget, *Clim. Past*, 3, 279–296, doi:10.5194/cp-3-279-2007, 2007b. 467, 471
- 5 Bretagnon, P. and Francou, G.: Planetary theories in rectangular and spherical variables – VSOP 87 solutions, *Astronomy and Astrophysics*, 202, 309–315, 1988. 466
- 10 Brovkin, V., Raddatz, T., Reick, C. H., Claussen, M., and Gayler, V.: Global biogeophysical interactions between forest and climate, *Geophys. Res. Lett.*, 36, L07405, doi:10.1029/2009GL037543, 2009. 466
- Davis, B. and Brewer, S.: Orbital forcing and role of the latitudinal insolation/temperature gradient, *Clim. Dynam.*, 32, 143–165, 2009. 470, 471, 482
- 15 Davis, B. A. and Stevenson, A. C.: The 8.2 ka event and Early-Mid Holocene forests, fires and flooding in the Central Ebro Desert, NE Spain, *Quaternary Sci. Rev.*, 26, 1695–1712, 2007. 472
- Davis, B. A. S., Brewer, S., Stevenson, A. C., Guiot, J., and Contributors, D.: The temperature of Europe during the Holocene reconstructed from pollen data, *Quaternary Sci. Rev.*, 22, 1701–1716, 2003. 470
- 20 Denton, G. H., Alley, R. B., Comer, G. C., and Broecker, W. S.: The role of seasonality in abrupt climate change, *Quaternary Sci. Rev.*, 24, 1159–1182, 2005. 465, 469
- Fischer, N. and Jungclauss, J. H.: Effects of orbital forcing on atmosphere and ocean heat transports in Holocene and Eemian climate simulations with a comprehensive Earth system model, *Clim. Past*, 6, 155–168, doi:10.5194/cp-6-155-2010, 2010. 467
- 25 Hibler, W.: Dynamic thermodynamic sea ice model, *Journal of Physical Oceanography*, 9, 815–846, 1979. 466
- Jungclauss, J. H., Keenlyside, N., Botzet, M., Haak, H., Luo, J. J., Latif, M., Marotzke, J., Mikolajewicz, U., and Roeckner, E.: Ocean circulation and tropical variability in the coupled model ECHAM5/MPI-OM, *J. Climate*, 19, 3952–3972, 2006. 466
- 30 Marsland, S. J., Haak, H., Jungclauss, J. H., Latif, M., and Roske, F.: The Max-Planck-Institute global ocean/sea ice model with orthogonal curvilinear coordinates, *Ocean Modelling*, 5, 91–127, 2003. 466
- Nesje, A., Matthews, J. A., Dahl, S. O., Berrisford, M. S., and Andersson, C.: Holocene glacier

Eemian and Holocene climate

N. Fischer and
J. H. Jungclauss

Title Page

Abstract

Introduction

Conclusions

References

Tables

Figures



Back

Close

Full Screen / Esc

Printer-friendly Version

Interactive Discussion



**Eemian and
Holocene climate**N. Fischer and
J. H. Jungclauss

Title Page

Abstract

Introduction

Conclusions

References

Tables

Figures

◀

▶

◀

▶

Back

Close

Full Screen / Esc

Printer-friendly Version

Interactive Discussion



fluctuations of Flatebreen and winter-precipitation changes in the Jostedalbreen region, western Norway, based on glaciolacustrine sediment records, *The Holocene*, 11, 267–280, 2001. 472

5 Otto, J., Raddatz, T., Claussen, M., Brovkin, V., and Gayler, V.: Separation of atmosphere-ocean-vegetation feedbacks and synergies for mid-Holocene climate, *Geophys. Res. Lett.*, 36, L09701, doi:10.1029/2009GL037482, 2009. 465, 470

Raddatz, T. J., Reick, C. H., Knorr, W., Kattge, J., Roeckner, E., Schnur, R., Schnitzler, K. G., Wetzels, P., and Jungclauss, J.: Will the tropical land biosphere dominate the climate-carbon cycle feedback during the twenty-first century?, *Clim. Dynam.*, 29, 565–574, 2007. 466

10 Raymo, M. E. and Nisancioglu, K.: The 41 kyr world: Milankovitch's other unsolved mystery, *Paleoceanography*, 18, 1011, doi:10.1029/2002PA000791, 2003. 471

Renssen, H., Seppa, H., Heiri, O., Roche, D. M., Goosse, H., and Fichefet, T.: The spatial and temporal complexity of the Holocene thermal maximum, *Nature Geoscience*, 2, 411–414, 2009. 465

15 Roeckner, E., Bäuml, G., Bonaventura, L., Brokopf, R., Esch, M., M., G., Hagemann, S., Kirchner, I., Kornblueh, L., Manzini, E., Rhodin, A., Schlese, U., Schulzweida, U., and Tompkins, A.: The atmospheric general circulation model ECHAM5. Part I: Model description., *Tech. Rep. Rep. 349*, 127 pp., Max Planck Institute for Meteorology, Available from MPI for Meteorology, Bundesstr. 53, 20146 Hamburg, Germany., 2003. 466

20 Semtner, A. J.: Model for thermodynamic growth of sea ice in numerical investigations of climate, *J. Phys. Oceanogr.*, 6, 379–389, 1976. 466

Wanner, H., Beer, J., Bütikofer, J., Crowley, T., Cubasch, U., Flückiger, J., Goosse, H., Grosjean, M., Joos, F., Kaplan, J., Küttel, M., Müller, S., Prentice, I., Solomina, O., Stocker, T., Tarasov, P., Wagner, M., and Widmann, M.: Mid- to Late Holocene climate change: an overview, *Quaternary Sci. Rev.*, 27, 1791–1828, 2008. 465

25 Wu, H., Guiot, J., Brewer, S., and Guo, Z.: Climatic changes in Eurasia and Africa at the last glacial maximum and mid-Holocene: reconstruction from pollen data using inverse vegetation modelling, *Clim. Dynam.*, 29, 211–229, 2007. 471

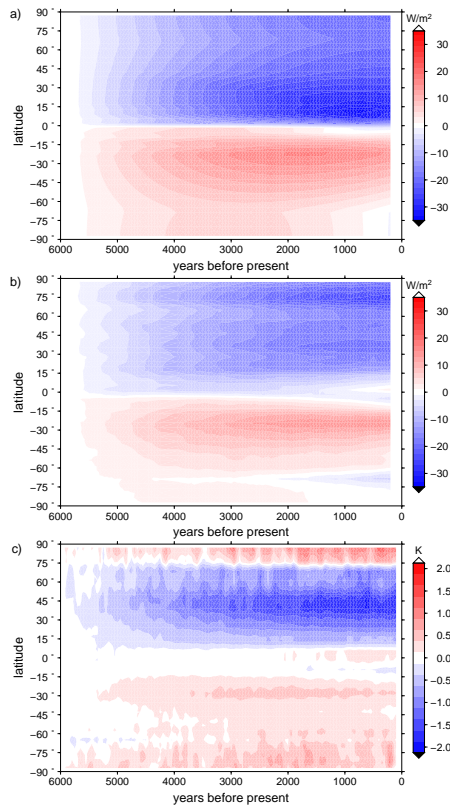


Fig. 1. Zonal mean Hovmoeller type diagrams of **(a)** seasonal insolation cycle amplitude (difference between yearly maximum and minimum insolation in W/m^2), **(b)** seasonal net insolation cycle amplitude (including planetary albedo), and **(c)** seasonal temperature cycle amplitude (difference between annual maximum and minimum zonal mean temperature). The panels show anomalies with respect to conditions at the mid-Holocene (mean of the first 100 years of the simulation).

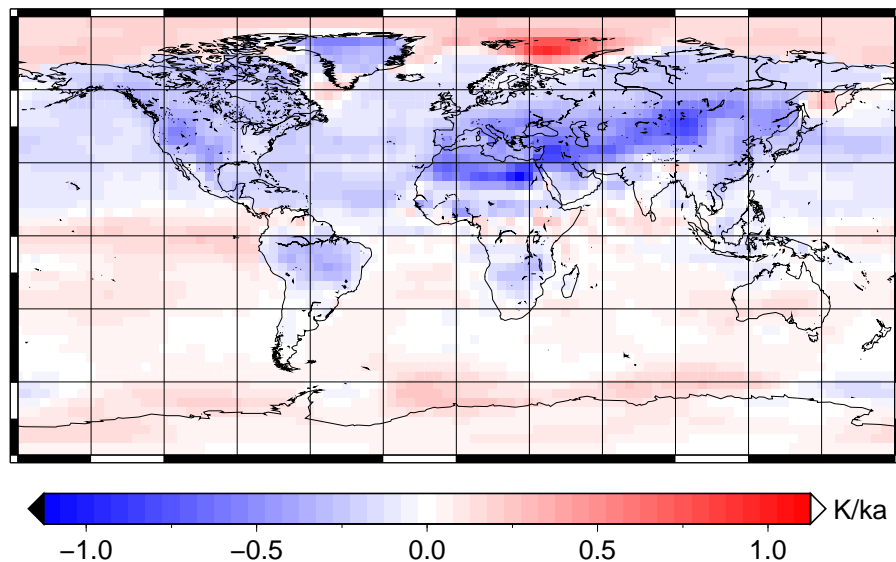
**Eemian and
Holocene climate**N. Fischer and
J. H. Jungclauss

Fig. 2. Linear trend in seasonal cycle amplitude (difference between warmest and coldest month) over the simulation period in K/ka – Kelvin per 1000 years.

[Title Page](#)[Abstract](#)[Introduction](#)[Conclusions](#)[References](#)[Tables](#)[Figures](#)[◀](#)[▶](#)[◀](#)[▶](#)[Back](#)[Close](#)[Full Screen / Esc](#)[Printer-friendly Version](#)[Interactive Discussion](#)

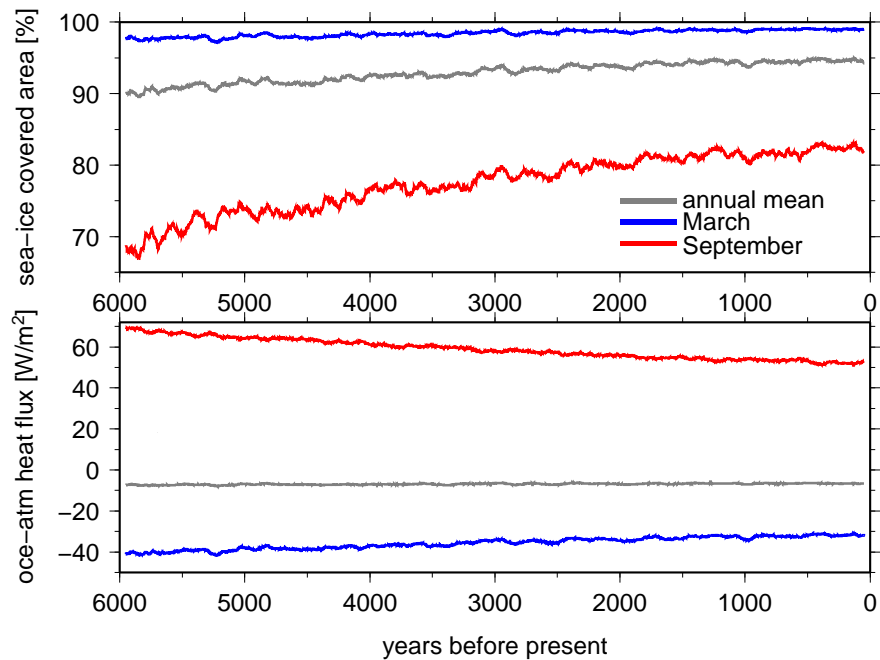


Fig. 3. Upper panel: percentage of sea-ice covered area in the Arctic Ocean, lower panel: atmosphere-ocean heat flux in W/m^2 – positive values from the atmosphere to the ocean. Both panels show 100 year running means

Eemian and Holocene climate

N. Fischer and
J. H. Jungclauss

Title Page

Abstract

Introduction

Conclusions

References

Tables

Figures

◀

▶

◀

▶

Back

Close

Full Screen / Esc

Printer-friendly Version

Interactive Discussion



Eemian and Holocene climate

N. Fischer and
J. H. Jungclauss

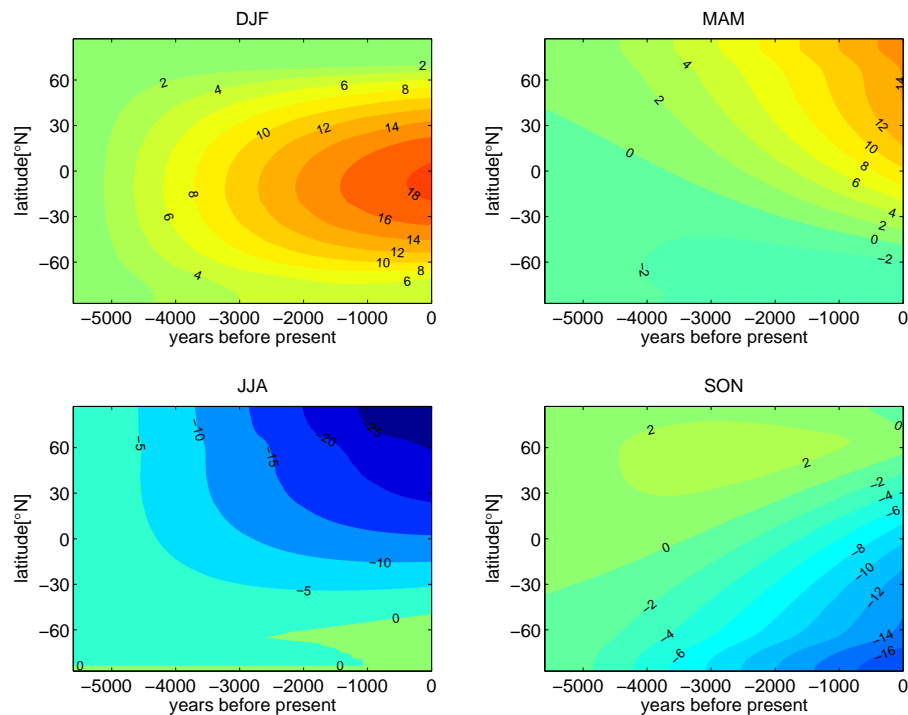


Fig. 4. Changes in seasonal insolation from the mid-Holocene to today in W/m² (winter – DJF, spring – MAM, Summer – JJA, autumn – SON). The reference is 6000 years before present.

Title Page

Abstract

Introduction

Conclusions

References

Tables

Figures

◀

▶

◀

▶

Back

Close

Full Screen / Esc

Printer-friendly Version

Interactive Discussion



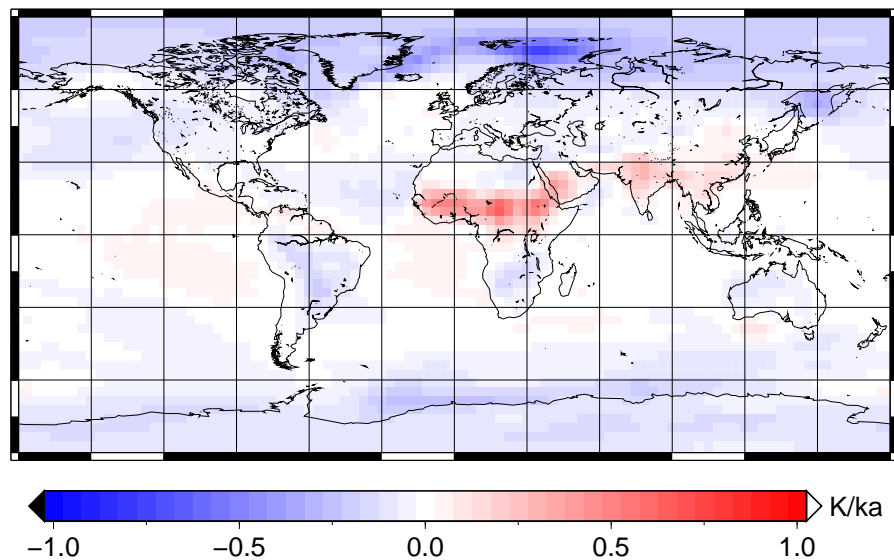
**Eemian and
Holocene climate**N. Fischer and
J. H. Jungclauss

Fig. 5. Linear trend in annual mean surface temperature over the simulation period in K/ka – Kelvin per 1000 years

Title Page

Abstract

Introduction

Conclusions

References

Tables

Figures

◀

▶

◀

▶

Back

Close

Full Screen / Esc

Printer-friendly Version

Interactive Discussion



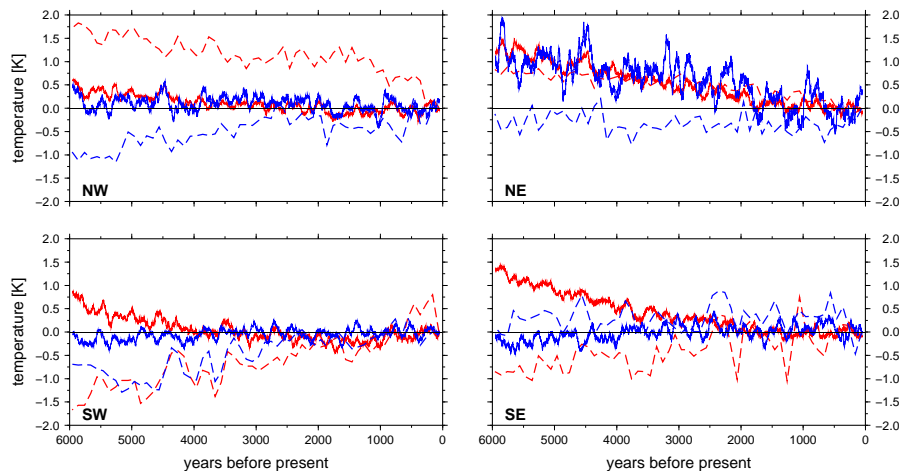
**Eemian and
Holocene climate**N. Fischer and
J. H. Jungclauss

Fig. 6. Comparison of seasonal temperature evolution between model results (solid lines) and reconstructions from pollen data (dashed lines) for northwestern (NW), northeastern (NE), southwestern (SW), and southeastern (SE) Europe – summer temperatures (red), winter temperatures (blue). Changes with respect to today's temperatures.

[Title Page](#)[Abstract](#)[Introduction](#)[Conclusions](#)[References](#)[Tables](#)[Figures](#)[⏪](#)[⏩](#)[◀](#)[▶](#)[Back](#)[Close](#)[Full Screen / Esc](#)[Printer-friendly Version](#)[Interactive Discussion](#)

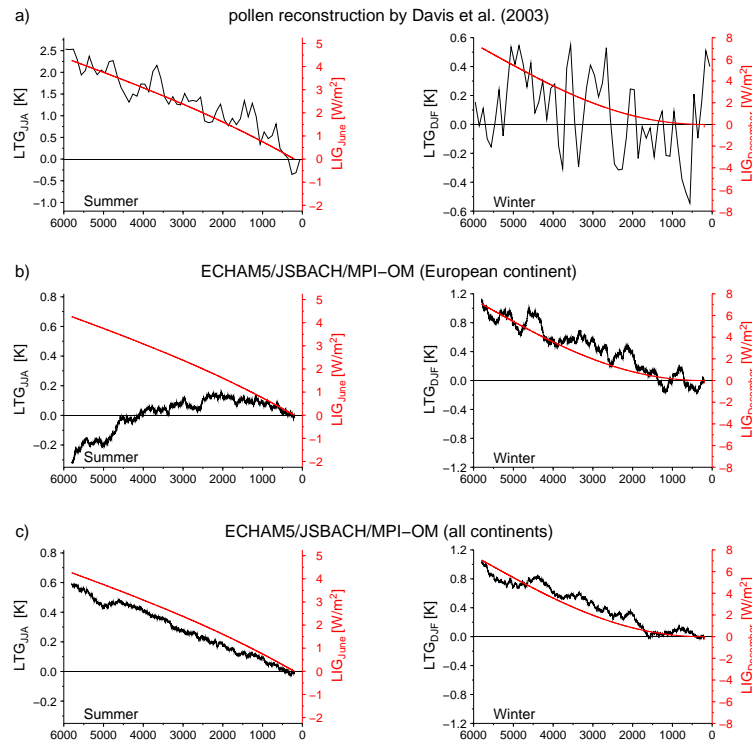
Eemian and
Holocene climateN. Fischer and
J. H. Jungclauss

Fig. 7. Seasonal latitudinal temperature gradients (in K, black lines, left y-axes) and June and December insolation gradients (in W/m^2 , red lines, right y-axes). Both defined as the difference between the latitude bands $30 - 45^\circ \text{N}$ and $55 - 75^\circ \text{N}$ in temperature and insolation, respectively. **(a)** temperature reconstruction from pollen (after Davis and Brewer (2009), subset of their Fig. 7), **(b)** corresponding model results for the European continent, and **(c)** model results for all continental land masses.

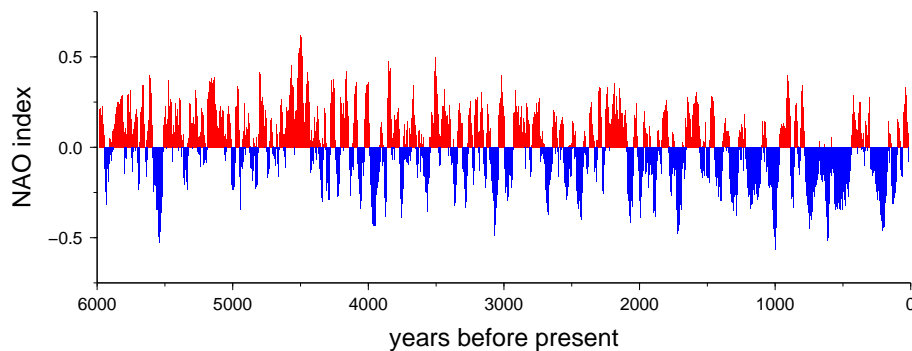
**Eemian and
Holocene climate**N. Fischer and
J. H. Jungclaus

Fig. 8. Time-series of North Atlantic Oscillation index calculated from the first EOF of winter mean sea level pressure over the North Atlantic region (30-year running mean).

Title Page

Abstract

Introduction

Conclusions

References

Tables

Figures

◀

▶

◀

▶

Back

Close

Full Screen / Esc

Printer-friendly Version

Interactive Discussion

